Applied Catalysis B: Environmental 176–177 (2015) 618–626

Contents lists available at ScienceDirect

Applied Catalysis B: Environmental

journal homepage: www.elsevier.com/locate/apcatb

Mn promoted $Pd/TiO_2–Al_2O_3$ catalyst for the selective catalytic reduction of NO_x by H_2

Kaijiao Duan [a], Biaohua Chen [a], Tianle Zhu [b], Zhiming Liu [a,*]

[a] State Key Laboratory of Chemical Resource Engineering, Beijing University of Chemical Technology, Beijing 100029, China
[b] School of Chemistry and Environment and Key Laboratory of Bio-Inspired Smart Interfacial Science and Technology of Ministry of Education, Beihang University, Beijing 100191, China

ARTICLE INFO

Article history:
Received 15 January 2015
Received in revised form 16 April 2015
Accepted 23 April 2015
Available online 24 April 2015

Keywords:
Nitrogen oxide
H_2-SCR
Pd–Mn catalyst

ABSTRACT

The performances of Mn modified $Pd/TiO_2–Al_2O_3$ catalysts for the selective catalytic reduction of NO_x by H_2 (H_2-SCR) were investigated in this study. The added Mn not only enhanced the activity but also remarkably increased N_2 selectivity above 150°C. Based on the characterization, it was found that Pd was present in the form of PdO and the synergetic effect between Pd and Mn led to more NO_x adsorbed and activated over Mn promoted $Pd/TiO_2–Al_2O_3$ catalyst. In situ DRIFTS studies demonstrated that the addition of Mn resulted in new types of adsorbed nitrite and nitrate species formed, both of which are reactive in the H_2-SCR process. Moreover, NH_3 and NH_x ($x = 0–2$) species adsorbed on Lewis acid sites were dominantly present instead of NH_4^+ species on Brønsted acid sites over the Mn modified $Pd/TiO_2–Al_2O_3$ catalyst. Therefore, the H_2-SCR of NO_x reaction was facilitated to proceed following the well-established NH_3-SCR reaction route.

© 2015 Elsevier B.V. All rights reserved.

1. Introduction

Selective catalytic reduction (SCR) has been regarded as one of the most effective methods to remove NO_x emitted from diesel engines. When hydrocarbon was used as the reducing agent (HC-SCR), the low-temperature activity of the catalyst needs to be improved [1,2]. In the NH_3-SCR of NO_x, besides the "NH_3 slip", the formed ammonium nitrate at low temperatures can occupy the active sites, and thus, result in activity loss of the catalyst [3,4]. Recently, H_2-SCR has attracted attention because in this process H_2 can efficiently reduce NO_x at low temperatures [5]. Another advantage of this technique is that the surplus hydrogen will react with oxygen to form water with zero pollution. For diesel powered vehicle, on-board hydrogen generation can be achieved by autothermal reforming (ATR) of diesel fuel [6]. Considering the on-board availability of hydrogen, H_2-SCR could be an alternative to NH_3-SCR for the reduction of NO_x.

Previous research showed that both Pt and Pd were active for the H_2-SCR of NO_x under learn-burn conditions [7–12]. Pd is less expensive and more abundant than Pt and the potential of Pd-based catalysts has not been fully exploited. For the reported Pd catalysts, their activity temperature windows were usually in the range of 100–200 °C [13,14]. The narrow temperature window can not guarantee the NO_x removal in the dynamic temperature of the exhaust due to the various engine operating conditions. In addition, the selectivity to N_2 also needs to be improved. Therefore, developing novel catalysts with high activity and N_2 selectivity in a broad operation temperature window is desired.

The combination of transition metal oxide with noble metal was an effective method to improve the catalytic performance of H_2-SCR catalyst. Leicht et al. [15] found that $Pd/WO_x/ZrO_2$ catalyst showed pronounced catalytic activity as well as high N_2 selectivity up to 80%. The addition of V_2O_5 to $1\%Pd/TiO_2–Al_2O_3$ led to an increased NO_x conversion and a wider activity temperature window [16]. The interaction between Pd and Cr contributed to enhancing the catalytic activity of Pd–Cr bimetallic catalyst for CO and NO removal [17]. The effects of Fe and Co on the performance of $Pd/Al_2O_3–TiO_2$ catalyst for H_2-SCR were also studied, and Co doping was found to improve N_2 selectivity [18]. However, to the best of our knowledge, no studies on Pd–Mn catalyst for the H_2-SCR of NO_x have been reported to date.

Park et al. [19] revealed that NH_x species adsorbed on the acid sites of manganese oxide were reactive in the H_2-SCR of NO_x over $Pt–MnO_x$ catalyst. The highly active $Pt/La_{0.5}Ce_{0.5}MnO_3$ catalyst in the temperature range 100–200 °C was also reported by Costa et al. [20]. Mn modified Pd (1 0 0) can form PdMn surface alloy [21], and NO dissociation at low temperature occurred on Mn atom, while NO decomposition at high temperature took place on Pd atom.

* Corresponding author. Tel.: +86 10 64427356.
E-mail address: liuzm@mail.buct.edu.cn (Z. Liu).

http://dx.doi.org/10.1016/j.apcatb.2015.04.048
0926-3373/© 2015 Elsevier B.V. All rights reserved.

Thus, the excellent catalytic activity in a wide temperature window was achieved. So the present work attempts to improve the catalytic performance of Pd catalyst for the H_2-SCR of NO_x by adding Mn. It was found that Mn addition to Pd/TiO_2–Al_2O_3 catalyst led to a noticeable promoting effect on the high-temperature activity and N_2 selectivity. The effect of H_2O on the H_2-SCR performance was also studied. Based on the characterization, the cause of the promoting effect of Mn has been elucidated.

2. Experimental

2.1. Catalyst preparation

Al_2O_3 was prepared by the sol–gel method as described in the literature [22]. TiO_2–Al_2O_3 support was synthesized by mixing Degussa AEROSIL TiO_2 P25 and the prepared Al_2O_3 at the mass ratio of 1:1. The mixture was added into deionized water, and then stirred at 40 °C for 4 h, followed by drying at 120 °C for 12 h. Pd–Mn/TiO_2–Al_2O_3 catalysts with 0.5%Pd and different Mn loadings were prepared by the incipient wetness method. After impregnating TiO_2–Al_2O_3 with a proper amount of manganese nitrate solution and drying at 120 °C, the sample was then impregnated with $PdCl_2$ solution. The obtained mixture was dried at 120 °C for 12 h. Finally, it was calcined at 500 °C for 4 h in air. For comparison, the 0.5%Pd/TiO_2–Al_2O_3 catalyst was also prepared by the same method as described above. The chlorine (Cl) on the surface of the catalyst was not detected by XPS analysis. Here-in-after, 0.5%Pd – *X*%Mn/TiO_2–Al_2O_3 (*X* = 1–5%) and 0.5%Pd/TiO_2–Al_2O_3 catalysts are denoted as Pd0.5Mn*X* and Pd0.5, respectively.

2.2. Activity measurements

The activity measurements were carried out in a fixed-bed quartz reactor using a 0.2 g catalyst of 40–60 mesh. A thermocouple was directly mounted inside the reactor and connected to a programmable temperature controller to monitor the reaction temperature. The feed gas was 0.25% NO, 1% H_2, 5% O_2, 0 or 5% H_2O, and He as the balance gas. The total flow rate was 200 mL min^{-1}, corresponding to a space velocity of 50,000 h^{-1}. The inlet and outlet gas concentrations of NO and NO_2 were analyzed by a chemiluminescence NO/NO_2 analyzer (Thermo Scientific, model 42i-HL). Meanwhile, the concentrations of NH_3 and N_2O were continually monitored by a FTIR spectrometer (Gasmet FTIR DX4000). All catalytic data were collected as the reaction was practically reached to a steady state at each temperature. The NO_x conversion, N_2 selectivity and NH_3 selectivity were calculated by the following equations, respectively.

$$NO_x \text{ conversion} = \frac{[NO_x]_{in} - [NO_x]_{out}}{[NO_x]_{in}} \times 100\% \quad (1)$$

$$N_2 \text{ selectivity} = \frac{[NO_x]_{in} - [NO_x]_{out} - 2[N_2O]_{out} - [NH_3]_{out}}{[NO_x]_{in} - [NO_x]_{out}} \times 100\% \quad (2)$$

$$NH_3 \text{ selectivity} = \frac{[NH_3]_{out}}{[NO_x]_{in} - [NO_x]_{out}} \times 100\% \quad (3)$$

In Eqs. (1)–(3), $[NO_x]_{in}$ and $[NO_x]_{out}$ represents the total concentration of NO and NO_2 in the inlet and outlet gas, respectively. Similarly, $[N_2O]_{out}$ and $[NH_3]_{out}$ represents the concentration of N_2O and NH_3 in the outlet gas.

2.3. Catalyst characterization

Characterization of the BET surface area of the samples was carried out with a Quantachrome Autosorb AS-1 system. Prior to the surface area measurement, the sample was degassed in vacuum at 400 °C for 4 h. X-ray diffraction (XRD) patterns were recorded on a Brucker D8 ADVANCE system using a Cu Kα radiation at 45 kV and 200 mA. The X-ray photoelectron spectroscopy (XPS) experiments were conducted on an ESCALab220i-XL electron spectrometer from VG Scientific using 300 W Mg Kα radiations. The fresh catalysts without pre-treatment were used in the characterization measurements. Binding energy (BE) was calibrated internally by carbon deposit C 1s at 284.8 eV.

Temperature-programmed desorption of NO_x (NO_x-TPD) experiments were carried out by using 0.2 g catalyst. The catalyst was pretreated in a flow of He at 400 °C for 1 h, and then cooled down to the room temperature, followed by the saturation with 0.25% NO + 5% O_2 at a flow rate of 100 mL min^{-1} for 1 h. After the sample was purged in He until no NO was detected, the TPD measurements were carried out up to 500 °C with the heating rate of 10 °C min^{-1} in flowing He. The desorbed NO_x were continuously monitored by the NO/NO_2 analyzer. Temperature-programmed reduction (H_2-TPR) experiments were conducted on a chemisorption analyzer (Micromeritics, ChemiSorb 2720 TPx) under a 5% H_2 gas flow (50 mL min^{-1}) at a rate of 10 °C min^{-1} up to 500 °C.

In-situ DRIFTS spectra were recorded using a thermo Nicolet 6700 spectrometer equipped with a high temperature environmental cell fitted with ZnSe window and a MCT detector cooled with liquid N_2. Prior to each experiment, the samples were pretreated under helium at a total flow rate of 100 mL min^{-1} for 60 min and

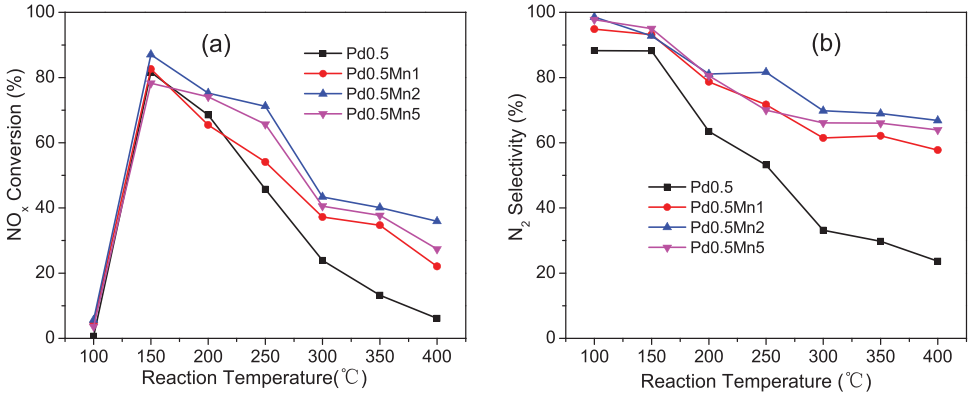

Fig. 1. H_2-SCR performances of Pd0.5 and Pd0.5Mn*X* with different Mn loadings. (a) NO_x conversion; (b) N_2 selectivity. Reaction conditions: *C*(NO) = 0.25%, *C*(H_2) = 1%, *C*(O_2) = 5%, He balance. GHSV = 50,000 h^{-1}.

then cooled to the desired temperature. A background spectrum was collected under a flowing He and was subtracted from the sample spectra. The DRIFTS spectra were recorded by accumulating 100 scans with a resolution of 4 cm^{-1}.

3. Results and discussion

3.1. H_2-SCR performances

The H_2-SCR performances of Pd0.5 and Pd0.5Mn*X* catalysts as a function of temperature are illustrated in Fig. 1. It is noticeable that both the NO_x conversion and N_2 selectivity of Mn modified Pd catalysts were enhanced above 150 °C. As shown in Fig. 1(a), NO_x conversion at high temperatures was improved with increasing Mn loading from 1% to 2%, while further increasing Mn loading to 5% led to a decreased NO_x conversion. From Fig. 1(b), it can be seen that the N_2 selectivity of Pd0.5Mn*X* catalysts were higher than that of Pd0.5 in the whole temperature region, and the promoting effect is significant above 200 °C. Small amounts of NH_3 were formed over the catalysts and the added Mn inhibited its formation (see Fig. S1). Therefore, the decrease of N_2 selectivity with increasing temperature is mainly due to the formation of more N_2O. Compared with Pd0.5 catalyst, more than 20% NO_x conversion and 30% N_2 selectivity were obtained over Pd0.5Mn2 catalyst above 200 °C. This fact indicates that the added Mn not only enhanced catalytic activity but also pronouncedly increased N_2 selectivity, and the optimum loading of Mn is 2%. Both the activity and N_2 selectivity of Pd0.5Mn2 catalyst are much higher than those of 1%Pd/TiO_2 and 1%Pd/Al_2O_3 catalysts reported previously [14]. The conversion of NO_x over Pd0.5Mn2 catalyst remains relatively constant as the time-on-stream is prolonged (see Fig. S2).

3.2. Effect of H_2O

The effect of H_2O on the NO_x conversion and N_2 selectivity of Pd0.5 and Pd0.5Mn2 catalysts was also investigated and the results are shown in Fig. 2. As shown in Fig. 2(a), the NO_x conversions over Pd0.5 and Pd0.5Mn2 catalysts were decreased below 200 °C in the presence of H_2O. Above 200 °C the conversion of NO_x over Pd0.5Mn2 was slightly decreased and the conversion over Pd0.5 was increased. The selectivity to N_2 over Pd0.5 catalyst is also increased above 200 °C due to the presence of H_2O. The positive effect of H_2O was also observed on Pt/MgO–CeO_2 catalyst [23]. Although the presence of H_2O leads to the decrease of the performance of Pd0.5Mn2 catalyst, its activity and selectivity to N_2 are still higher than those obtained over Pd0.5 catalyst. This is very important for the potential deNO_x application.

Table 1
Textural properties of Pd0.5 and Pd0.5Mn2 catalysts.

Catalyst	BET area ($m^2\ g^{-1}$)	Pore volume ($cm^3\ g^{-1}$)	Pore size (nm)
Pd0.5	128	0.48	10.9
Pd0.5Mn2	136	0.41	9.3

3.3. Effects of H_2 and O_2 concentrations

The effects of H_2 and O_2 concentrations on the H_2-SCR performance of Pd0.5Mn2 catalyst at 200 °C in the presence of H_2O were investigated and the results are presented in Fig. 3. It showed that NO_x conversion was obviously increased when H_2 concentration increased from 0.25% to 1%, and further increasing to 2% led to a slightly increased NO_x conversion. In contrast, the N_2 selectivity gradually decreased as H_2 concentration increased. From Fig. 3(b), it can be seen that the increase of O_2 concentration led to a decrease of NO_x conversion, especially, with a sharp drop of 30% when more than 5% O_2 was employed in the feed gas. These facts are similar to the results observed on Pt/MgO–CeO_2 catalyst [24]. Increasing O_2 concentration from 1 to 5% enhanced N_2 selectivity, and then the further increase of O_2 concentration exhibited little impact on the N_2 selectivity, which is similar to the results of Pt/WO_3/ZrO_2 catalyst [25].

3.4. Catalyst characterization

3.4.1. BET surface area and XRD patterns

BET results of Pd0.5 and Pd0.5Mn2 catalysts are presented in Table 1. As it can be seen, the addition of Mn to Pd led to an increased surface area but decreased pore volume and pore size. The large surface area of Pd0.5Mn2 catalyst may favor the H_2-SCR to proceed.

From the XRD patterns of Pd0.5 and Pd0.5Mn2 catalysts (not shown), only the peaks of Al_2O_3 and anatase and rutile form of TiO_2 appeared. Neither Pd nor PdO peaks were observed over the two catalysts. The peaks ascribed to MnO_x phases were absent on Pd0.5Mn2 catalyst, indicating that manganese oxide was highly dispersed on the surface of the catalyst.

3.4.2. NO_x-TPD

NO_x-TPD profiles over Pd0.5 and Pd0.5Mn2 catalysts are illustrated in Fig. 4. It can be seen that the amount of desorbed NO_x, NO_2 and NO were pronouncedly increased with the addition of Mn, indicating that more NO_x adsorbed on Pd0.5Mn2 catalyst. In the case of Pd0.5Mn2 catalyst, 41.1 μmol g_{cat}^{-1} and 27.1 μmol g_{cat}^{-1} desorbed NO_x and NO_2 were achieved, which were 1.7 and 1.5 times higher than that obtained on Pd0.5 catalyst. Besides, it is well worth

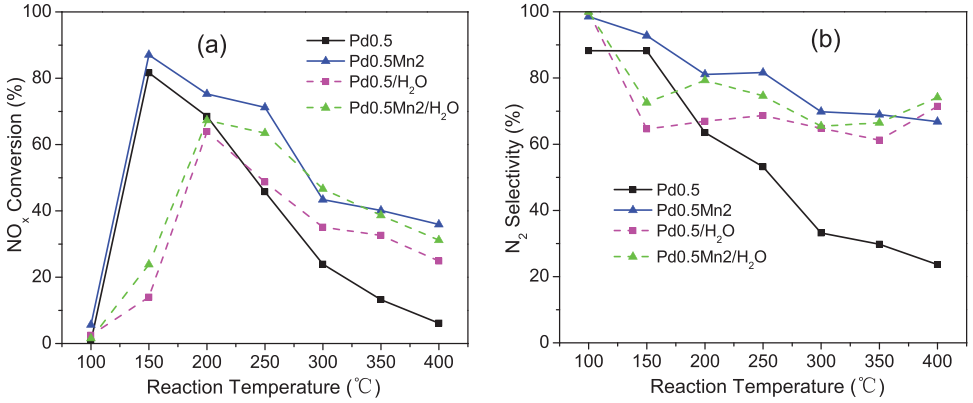

Fig. 2. H_2-SCR performances of Pd0.5 and Pd0.5Mn2 catalysts in the presence of H_2O. (a) NO_x conversion; (b) N_2 selectivity. Reaction conditions: $C(NO) = 0.25\%$, $C(H_2) = 1\%$, $C(O_2) = 5\%$, $C(H_2O) = 5\%$, He balance. GHSV = 50,000 h^{-1}.

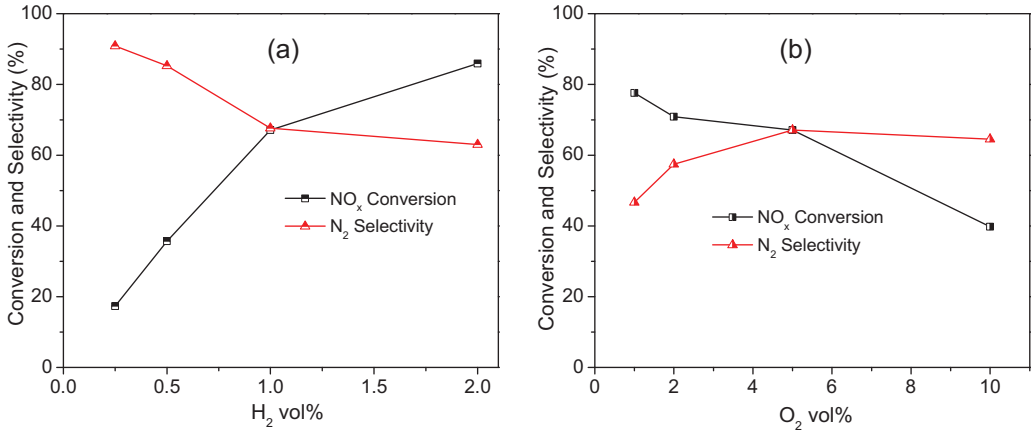

Fig. 3. Effects of H_2 (a) and O_2 (b) concentrations on H_2-SCR performance of Pd0.5Mn2 catalyst at 200 °C. Reaction conditions: $C(NO) = 0.25\%$, $C(H_2) = 0–2\%$, $C(O_2) = 0–10\%$, 5% H_2O, He balance. GHSV = 50,000 h^{-1}.

noting that the ratio of NO_2 to NO_x was increased from 65.8% on Pd0.5 to 78.7% on Pd0.5Mn2, suggesting that both the adsorption capability and the ability to oxidize NO to NO_2 were promoted due to the introduction of Mn. It was reported that the reaction rate of $H_2 + NO_2$ was much faster than that of $H_2 + NO$, so the more NO_x were adsorbed on catalyst the higher activity and selectivity were achieved [9,26]. There were two small NO_x desorption peaks observed on Pd0.5 catalyst, one centered at 90 °C and the other centered at 420 °C. While on Pd0.5Mn2 catalyst three strong NO_x desorption peaks at 80, 200 and 260 °C appeared, indicating that there were new adsorbed species with different thermal stability formed due to the added Mn. The significantly lowered desorption temperature indicated that the adsorbed NO_x was less stable on Pd0.5Mn2 surface than that on Pd0.5 catalyst surface. Costa et al. [27] suggested whether adsorbed species on catalyst surface promptly participate in $NO + O_2 + H_2$ reaction was critical to obtain high catalytic performance. Consequently, the less stable adsorbed NO_x over Pd0.5Mn2 catalyst surface could be responsible for the high NO_x conversion and N_2 selectivity.

3.4.3. XPS

Fig. 5 illustrates Pd 3d, Mn 2p and O 1s XPS spectra obtained from Pd0.5 and Pd0.5Mn2 catalysts. In Fig. 5(a), the lower intensity of Pd 3d on Pd0.5Mn2 surface suggested that Pd surface concentration decreased after the Mn addition, and the result is shown in Table 2. By performing a peak fitting deconvolution, the Pd 3d spectra of Pd0.5 catalyst can be separated into two characteristic peaks centered at 334.7 and 336.1 eV, which were ascribed to metallic Pd and PdO [28,29], respectively (see Fig. 5(a)). For Pd0.5Mn2,

Table 2
Atomic concentrations (%) on the surface of the catalysts determined by XPS.

Catalyst	Pd	Mn	O_α/O^a
Pd0.5	0.36	–	63.3
Pd0.5Mn2	0.21	1.23	76.5

[a] O is composed of lattice oxygen (O_β) and surface chemisorbed oxygen (O_α).

only the peak of 336.6 eV corresponding to PdO was present. PdO was reported to be the predominant active sites of Pd catalyst for $NO + H_2 + O_2$ reaction above 200 °C [13,30], therefore, the presence of PdO on Pd0.5Mn2 surface favored the high-temperature H_2-SCR reaction. The drop of Pd surface concentration on Pd0.5Mn2 catalyst probably resulted from the synergetic interaction between Pd and Mn, which could decrease the binding energy of NO_x with the surface of Pd0.5Mn2 catalyst as elucidated in the NO_x-TPD profile.

In Fig. 5(b), the typical Mn 2p spectra of Pd0.5Mn2 located at 641.5 and 653.3 eV indicated the existence of mixed-valence manganese system (Mn^{3+} and Mn^{4+}) [31]. The peak with the binding energy of 645.4 eV ascribed to Mn^{2+} [32] was also observed. It is evident that Mn^{3+} is the predominant form with the high ratio of 46.3% ($Mn^{3+}/(Mn^{2+} + Mn^{3+} + Mn^{4+})$). Ettireddy et al. [33] reported that NO_x was prone to adsorbing as nitrate and/or nitrite on MnO_2 and Mn_2O_3. Hence, the gathered MnO_xon Pd0.5Mn2 surface led to the more adsorbed NO_x on the catalyst, as shown in the NO_x-TPD profiles. O 1s XPS spectra of Pd0.5 and Pd0.5Mn2 are displayed in Fig. 5(c). Both of them presented two distinct peaks: one located at 529.5–529.7 eV can be ascribed to lattice oxygen (denoted as O_β), and the other one at 531.5–531.6 eV can be assigned to surface

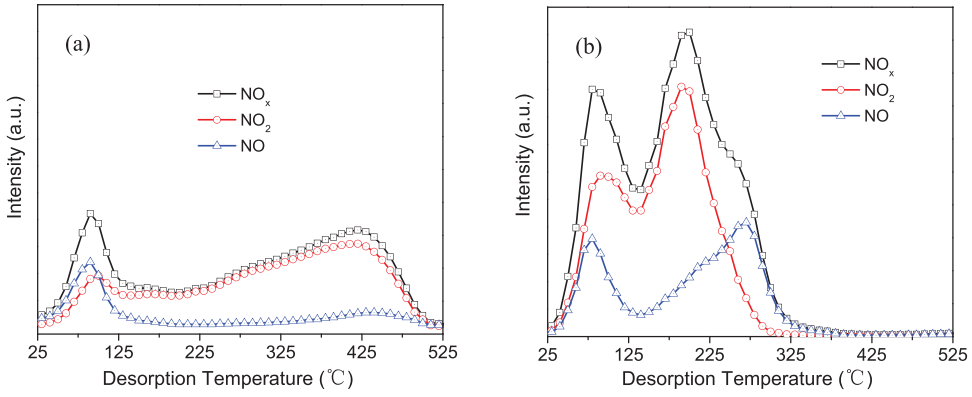

Fig. 4. NO_x-TPD profiles over Pd0.5 (a) and Pd0.5Mn2 (b) catalysts.

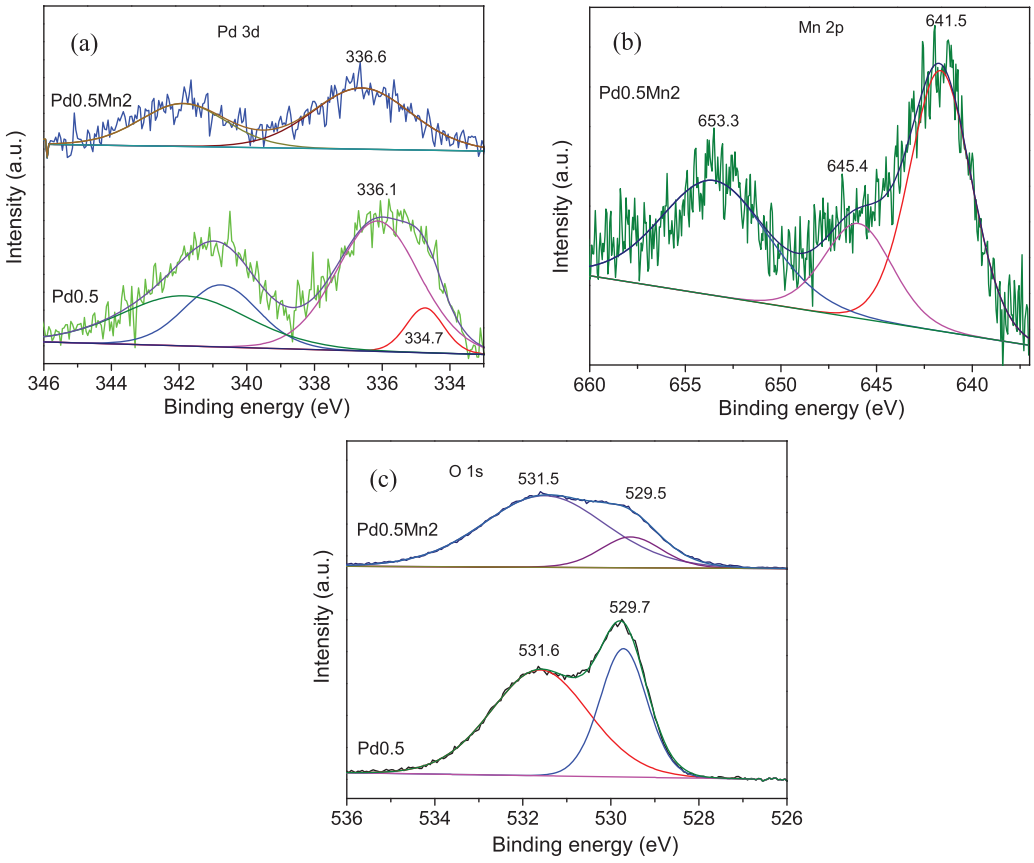

Fig. 5. XPS spectra of Pd 3d (a), Mn 2p (b) and O 1s (c) for Pd0.5 and Pd0.5Mn2 catalysts.

chemisorbed oxygen (denoted as O_α). It is interesting to note that the ratio of O_α/O greatly increased after the addition of Mn, suggesting that the amount of oxygen vacancy was increased on Pd0.5Mn2 catalyst. Amores et al. [34] reported that the surface chemisorbed oxygen contributed to the adsorption and oxidation of NO to NO_2, which was favorable to be reduced by hydrogen in the SCR process.

3.4.4. H_2-TPR

Fig. 6 showed the H_2-TPR profiles of Pd0.5 and Pd0.5Mn2 catalysts. One peak centering at 115 °C can be observed on Pd0.5 catalyst, and this peak can be assigned to the reduction of PdO. For Pd0.5Mn2 catalyst, three reduction peaks at 165, 220 and 390 °C appeared. Ettireddy et al. [33] reported that three H_2 reduction peaks on MnO_x/TiO_2 were attributed to MnO_2 to Mn_2O_3 at 282 °C, Mn_2O_3 to Mn_3O_4 at 348 °C and Mn_3O_4 to MnO at 432 °C, respectively. Apparently, the co-presence of Pd and Mn on Pd0.5Mn2 catalyst significantly lowered the reduction temperature of MnO_x, indicating that $MnO_x$was easily reduced by activated H atom on the surface of Pd. In the H_2-SCR process MnO_x is prone to changing its oxidation state under the reaction condition, whilst hydrogen is inherently activated through dissociation on Pd surface. Therefore, the co-presence of Pd and Mn on Pd0.5Mn2 catalyst significantly induced the oxygen vacancies on MnO_x, which is beneficial for the adsorption of NO_x and oxygen and then facilitated the H_2-SCR reaction. In turn, the removal rate of adsorbed hydrogen on Pd was increased, leaving more vacant Pd sites to adsorb and activate H_2 molecules, thus, leading to the enhanced activity and N_2 selectivity. These facts suggested that the co-existence of Pd and Mn led to a synergetic effect and improved the reducibility of the catalyst. High temperature favors the hydrogen activation on Pd surface, hence, the synergetic effect was obvious above 200 °C. In addition, the reduction temperatures at 165 and 220 °C shown in Fig. 6 seemed to be far below the value expected. The first one was supposed to be due to the co-reduction of palladium oxide and surface Mn^{4+}, and the second one was probably due to the reduction of Mn_2O_3 to Mn_3O_4 coordinated with Pd atom, further suggesting the synergetic effect between Pd and Mn.

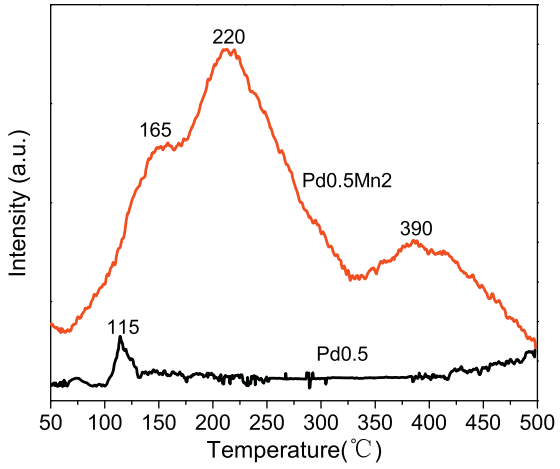

Fig. 6. H_2-TPR profiles of Pd0.5 and Pd0.5Mn2 catalysts.

3.5. *In situ DRIFTS studies*

3.5.1. *Co-adsorption of NO and O_2*

Fig. 7 shows the DRIFT spectra of NO + O_2 on Pd0.5 and Pd0.5Mn2 catalysts at different temperatures. As illustrated in Fig. 7(a), the exposure of Pd0.5 catalyst to a NO + O_2 gas flow caused the appear-

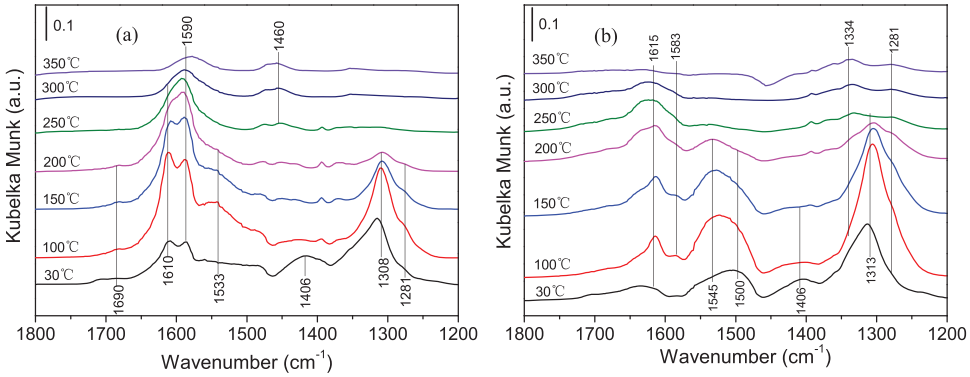

Fig. 7. In situ DRIFTS spectra of NO + O_2 adsorption on Pd0.5 (a) and Pd0.5Mn2 (b) catalysts at different temperatures. Conditions: C(NO) = 0.25%, C(O_2) = 5%, He balance.

ance of bands at 1281, 1308, 1406, 1533, 1590, 1610 and 1690 cm^{-1}, which were ascribed to monodentate nitrate (1281 and 1406 cm^{-1}) [9,35], chelating bidentate nitrate (1308, 1533 and 1590 cm^{-1}) [36,37], asymmetric vibration mode of adsorbed NO_2 (1610 cm^{-1}) [38] and a bent mono-nitrosyl adsorbed on Pd^0 (1690 cm^{-1}) [39], respectively. The peak ascribed to monodentate nitrate vanished with increasing temperature up to 200 °C. Further increasing temperature led to new band appeared at 1460 cm^{-1}, which was ascribed to monodentate nitro specie on the support [9], indicating that monodentate nitrates were unstable on Pd0.5 catalyst.

Fig. 7(b) shows the in situ DRIFTS spectra of adsorbed nitrogen oxide species on Pd0.5Mn2 catalyst. Apparently, the introduction of Mn led to two new bands appeared: one at 1334 cm^{-1} was attributed to chelating bidentate nitrite bound to MnO_x through an oxygen atom [19] and the other at 1500 cm^{-1} was assigned to monodendate nitrate [37]. The intensities of the peaks at 1281 and 1313 cm^{-1} were stronger than those on Pd0.5 catalyst. Moreover, the bands of chelating bidentate nitrate (1313 and 1545 cm^{-1}) and asymmetric vibration mode of adsorbed NO_2 (1615 cm^{-1}) showed blue shifts. Therefore, addition of Mn to Pd0.5 not only induced new species formed on MnO_x but also led to more species adsorbed on the catalyst, as well as lowered their binding energy (thermal stability). As temperature increased to 200 °C the intensities of all bands decreased but they did not disappear. The peak ascribed to mono-nitrosyl species on Pd^0 was not observed, indicating Pd^0 was absent on Pd0.5Mn2, which was consistent with the XPS results.

3.5.2. *Reaction of H_2 and NO_x*

Fig. 8 shows the dynamic changes of in-situ DRIFT spectra of adsorbed species over Pd0.5 and Pd0.5Mn2 catalysts at 200 °C. Fig. 8(a) shows that on Pd0.5 catalyst after the gas flow switch to H_2, nitrates and nitrosyl species (at 1281, 1308, 1533, 1610 and 1690 cm^{-1}) gradually disappear, whilst strong bands at 1409, 1504, 1638 and 1681 cm^{-1} are presented, which are attributed to symmetric and asymmetric bending vibrations of NH_4^+ species adsorbed on Brønsted acid sites (1409 and 1681 cm^{-1}) [37], monodentate nitrate (1504 cm^{-1}) and adsorbed water (1638 cm^{-1}) [36], respectively. This indicated a strong combustion reaction of hydrogen and oxygen over Pd0.5 catalyst. Again, when the gas flow switched to NO + O_2, the active intermediates appeared again accompanied by the disappearance of NH_4^+ species adsorbed on Brønsted acid sites. This fact indicates that besides nitrate species NH_4^+ species were essential for the H_2-SCR of NO_x over Pd0.5 catalyst.

As illustrated in Fig. 8(b), over Pd0.5Mn2 catalyst after the introduction of H_2 more nitrates and nitrites (at 1281, 1313, 1500, 1545, 1583 and 1615 cm^{-1}) disappeared and the disappearing rate was much faster (within 10 min) than that on Pd0.5 catalyst (within 20 min). The absence of 1334 cm^{-1} was due to the overlaping with the peak at 1313 cm^{-1}, indicating that new species formed on MnO_x and the support was active for the H_2-SCR reaction. At the same time, a new band at 1600 cm^{-1} assigned to asymmetric bending vibration of NH_x (x = 0–2) adsorbed on Lewis acid site [38] was observed, suggesting that NH_x species was critical intermediate in NO + H_2 + O_2 reaction over Pd0.5Mn2 catalyst. It is worth to note that the band intensity of adsorbed water was much weaker compared with that on Pd0.5 catalyst, indicating that the combustion reaction of hydrogen and oxygen on Pd0.5Mn2 catalyst was suppressed. After switching H_2 to NO + O_2 again, different adsorbed nitrogen oxide species with strong intensity appeared as well as the disappearance of NH_x species, further confirming the distinction of NO + H_2 + O_2 reaction route between Pd0.5 and P0.5Mn2 catalysts.

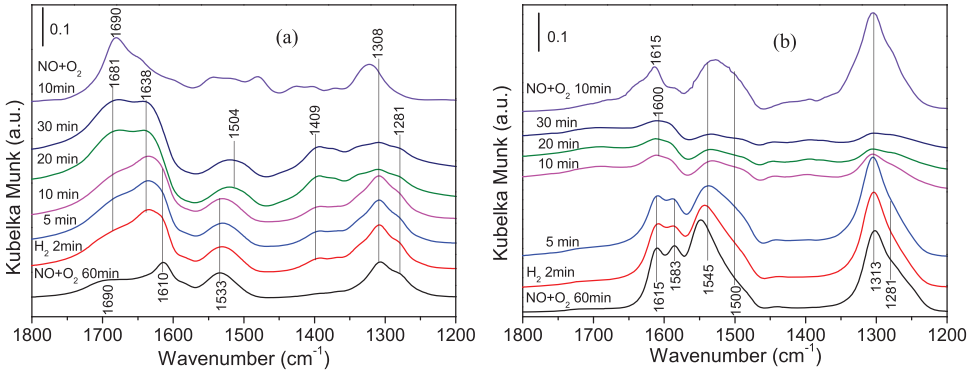

Fig. 8. In situ DRIFTS spectra of surface species adsorbed on Pd0.5 (a) and Pd0.5Mn2 (b) exposure to 0.25%NO + 5%O_2 mixed gas followed by H_2 gas, and then switched to 0.25%NO + 5%O_2 mixed gas again at 200 °C. Conditions: C(NO) = 0.25%, C(H_2) = 1%, C(O_2) = 5%, He balance.

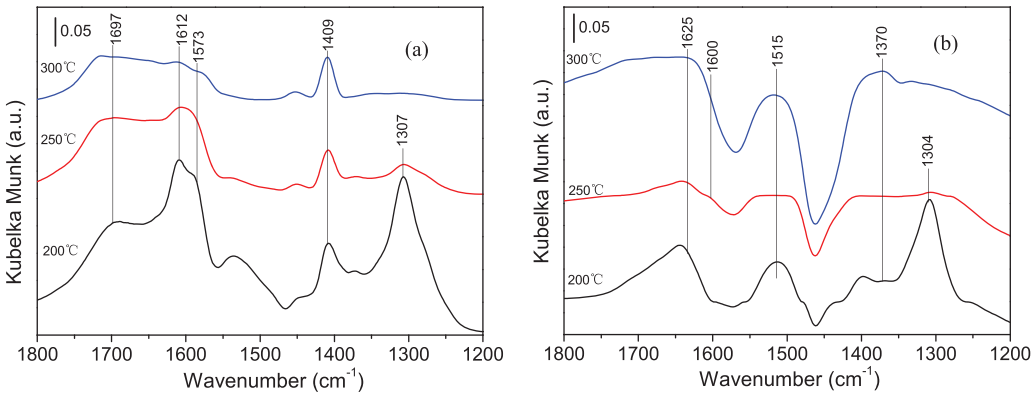

Fig. 9. In situ DRIFTS spectra of surface species in the steady state over Pd0.5 (a) and Pd0.5Mn2 (b) catalyst in the flow of 0.25%NO + 1%H_2 + 5%O_2. Conditions: C(NO) = 0.25%, C(H_2) = 1%, C(O_2) = 5%, He balance.

3.5.3. *DRIFTS under NO+O_2+H_2*

Fig. 9 shows the in-situ DRIFT spectra of adsorbed species over Pd0.5 and Pd0.5Mn2 catalysts in the flow of 0.25%NO + 1%H_2 + 5%O_2 at various temperatures. After an the exposure of Pd0.5 catalyst to NO + H_2 + O_2 at 200 °C, some peaks ascribed to chelating bidentate nitrate (1307 and 1573 cm^{-1}) [36,37], NH_4^+ adsorbed on Brønsted acid site (1409 cm^{-1}) [34], asymmetric vibration mode of adsorbed NO_2 (1612 cm^{-1}) [38] and a bent mono-nitrosyl adsorbed on Pd^0 (1697 cm^{-1}) [39], respectively, were observed (see Fig. 9(a)). With increasing temperature, the intensity of the peak assigned to chelating bidentate nitrate decreased, while those related to NH_4^+ species increased. As shown in Fig. 9(b), the DRIFT spectra of adsorbed species over Pd0.5Mn2 catalyst are different from those of Pd0.5 catalyst. Besides the bands to monodentate nitrate (1515 cm^{-1}) [37] and chelating bidentate nitrate (1304 cm^{-1}) appeared, the peaks assigned to the adsorbed NH_3 (1370 cm^{-1}) and NH_x species (1600 and 1625 cm^{-1}) [38] also presented. This fact indicates that the formation of NH_3 and NH_x species plays an important role in NO + H_2 + O_2 reaction over Pd0.5Mn2 catalyst. It should be mentioned that several of the observed IR bands may reflect inactive species, and only SSTIKA (steady-state transient isotopic kinetic analysis) combined with DRIFTS could resolve this [9].

3.5.4. *NH_3 adsorption*

Acid site change resulted from Mn addition on Pd0.5Mn2 was studied by exposing Pd0.5 and Pd0.5Mn2 to NH_3 with increasing temperatures. Fig. 10(a) shows the ammonia species adsorbed over Pd0.5 catalyst. Below 200 °C, the typical adsorbed NH_3 (1377 cm^{-1}) and asymmetric and symmetric bending vibrations of NH_4^+ species adsorbed on Brønsted acid sites (1428, 1652, 3063, and 2882 cm^{-1}) [34–36] appeared. The weak peaks attributed to asymmetric bending vibration of NH_x (x = 0–2) adsorbed on Lewis acid site (at 1600 cm^{-1}) and adsorbed water (at 1630 cm^{-1}) also appeared. As the temperature increased to 350 °C, the intensities of the bands at 1600 and 1652 cm^{-1} gradually decreased, accompanied by the appearance of four peaks at 1331, 1396, 1485 and 3129 cm^{-1}, which was attributed to asymmetric and symmetric bending vibrations of NH_4^+ species adsorbed on Brønsted acid sites [34,40]. It is clear that Brønsted acid sites were predominant over Pd0.5 catalyst in the temperature range of 30–350 °C.

The DRIFT spectra of NH_3 adsorption on Pd0.5Mn2 catalyst also showed asymmetric and symmetric bending vibrations of NH_4^+ species adsorbed on Brønsted acid sites (3143, 2917, and 1445 cm^{-1}) [37,40], however, all of them were much weaker than that on Pd0.5 catalyst (see Fig. 10(b)). And the strong bands assigned to adsorbed NH_3(1384 cm^{-1}) and asymmetric bending vibration of NH_x (x = 0–2) adsorbed on Lewis acid site (1594 cm^{-1}) appeared, suggesting that adsorbed NH_3 was stable on Pd0.5Mn2 catalyst and Lewis acid sites were dominantly present. With increasing temperature the intensities of all bands decreased, but those at 1594 and 1384 cm^{-1} was still strong from 30 to 350 °C. This fact indicated that the dominant acid sites of Pd0.5Mn2 catalyst were transformed from Brønsted acid to Lewis acid due to the addition of Mn.

According to the in situ DRIFTS results as described above, more active nitrogen-containing intermediates formed on Pd0.5Mn2 catalyst and some of the peaks occurred blue shift (see Fig. 7), suggesting the decreased binding energy of the adsorbed NO_x species with the surface of Pd0.5Mn2, on which the species was unstable and prone to reacting with the activated H atoms. More importantly, new types of adsorbed nitrite and nitrate species on MnO_x and the support were formed (at 1334 and 1500 cm^{-1}) and both of them were essentially active in the H_2-SCR process. Indeed

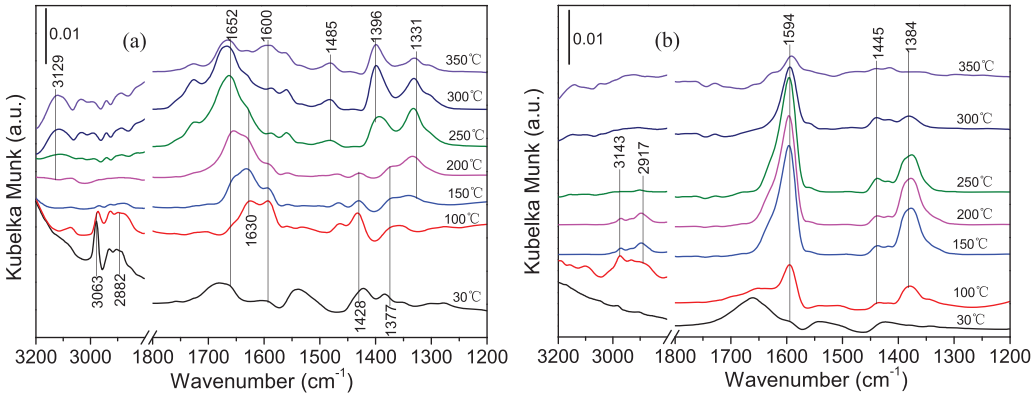

Fig. 10. In situ DRIFTS spectra of NH_3 adsorption on Pd0.5 (a) and Pd0.5Mn2 (b) catalysts at different temperatures. Conditions: C(NH_3) = 0.05%, He balance.

compared with Pd0.5 catalyst, the faster reaction rate of H_2 with $NO + O_2$ on Pd0.5Mn2 catalyst (see Fig. 8) revealed that adsorbed nitrogen oxides were prone to being reduced by the dissociated hydrogen spillover from Pd surface. Costa and Efstathiou [9] summarized the factors that control the H_2-SCR of NO_x activity and N_2 selectivity on Pt/MgO–CeO_2 catalyst and pointed out that the structure of adsorbed NO_x and their binding energy with catalyst was very important. The relatively weaker binding energy of adsorbed NO_x with catalyst contributed to the desirable reaction with H atom and inhibited the activated H atom consumption by excess oxygen, thus leading to more vacant active Pd sites occupied by hydrogen and facilitating the $NO + H_2 + O_2$ reaction. H-spillover was reported to play an important role in the H_2-SCR of NO_x [11,23]. The synergetic effect between Pd and Mn could promote the H-spillover from Pd to Mn and the support, resulting in the faster reaction rate of H_2 with adsorbed NO_x (see Fig. 8). Therefore, after Mn addition, those new and more highly active nitrogen-containing species with comparatively lower binding energy with Pd0.5Mn2 catalyst and the promoted H-spillover process are responsible for the high activity and remarkable N_2 selectivity at high temperatures.

On the other hand, in situ DRIFTS spectra of Pd0.5Mn2 catalyst also demonstrated that in the H_2-SCR process adsorbed NH_3 and NH_x ($x = 0–2$) species adsorbed on Lewis acid sites were two important intermediate species, which substituted for NH_4^+ species on Pd0.5 catalyst. NH_3 adsorption experiment further confirmed that the predominant acid sites transformed from Brønsted acid sites on Pd0.5 catalyst to Lewis acid sites on Pd0.5Mn2 catalysts. Currently, mainly two H_2-SCR of NO mechanisms are proposed: NO adsorption/dissociation mechanism and oxidation-reduction mechanism [5,11], and the latter is preferable for high-temperature $NO + H_2 + O_2$ reaction. For oxidation-reduction mechanism, NH_4^+ on Brønsted acid sites, adsorbed NH_3 and NH_x ($x = 0–2$) species on Lewis acid sites are critical active intermediates. It is believed that if NH_3 formation rate as well as NH_x ($x = 0–2$) generation rate is increased, N_2 formation will be expected to increase through the NH_3-SCR reaction pathway [41,42]. The study of low-temperature and high-temperature H_2-SCR mechanisms on Pd/TiO_2/Al_2O_3 catalyst revealed that the presence of NH_x on Lewis acid sites at high temperature favored high activity and N_2 selectivity [30]. The formed NH_3 over Pt–MnO_x catalyst seems to be the more favorable intermediate for N_2 selectivity [19]. Nanba et al. [41] elucidated that the observed NH_3 in H_2-SCR reaction was further involved in the selective reduction of NO and was effectively converted to N_2. Besides, NH_4^+ or adsorbed NH_3 and NH_x species formation greatly depended on the support acidity, which was the key factor controlling N_2 selectivity for H_2-SCR [43]. Yazawa et al. [44,45] suggested that the highly electrophilic property of support was beneficial for the high activity and N_2 selectivity. It is well known that Brønsted acid site is of highly electrophobic while Lewis acid site is liable to be electrophilic. Consequently, it is proposed that the predominant Lewis acid sites on Pd0.5Mn2 catalyst led to the formation of adsorbed NH_3 and NH_x ($x = 0–2$) species at high temperature and then considerably promoted the N_2 selectivity by NH_3-SCR process. In addition, since the adsorbed NH_4^+ species on Brønsted acid sites originated from the migration of NH_3 and NH_x ($x = 0–2$) from active sites, the reaction of NH_3/NH_x with NO_x should be faster than NH_4^+ with NO_x. Therefore, the in situ DRIFTS results account for the high catalytic performance of Pd0.5Mn2 catalyst.

H_2 in the reactant gas can reduce palladium oxide and to keep Pd^0 or Pd_2O form, and also as a reactant to participate in the formation of NH_x species, as well as to lower the binding energy of Pd and NO molecule. However, most of hydrogen is consumed by oxygen instead of participating in NO–H_2 reaction at high temperature, thus leading to a decreased activity. Hence, the enhanced activity and suppressed activity caused by increasing hydrogen concentration and oxygen concentration over Pd0.5Mn2 catalysts are observed in Fig. 3.

Metallic Pd is active for low-temperature H_2-SCR of NO_x and PdO works as primary active sites for high-temperature $NO + H_2 + O_2$ reaction, and over Pd0.5Mn2 catalyst the only PdO form was observed. Moreover, the co-presence of Mn^{3+} and Mn^{4+} and the increased oxygen vacancy over Pd0.5Mn2 catalyst led to the high capacity of NO adsorption and the high capability to oxidize NO to NO_2, both of which are responsible for the enhanced activity of Pd0.5Mn2 catalyst. The considerably promoted N_2 selectivity of Pd0.5Mn2 catalyst at high temperature can be attributed to these consequences from Mn addition: the first one is the lowered binding energy of nitrogen oxides species with MnO_x and the support surface, which induced the fast $NO + H_2 + O_2$ reaction; the second one is the transformed predominant Lewis acid sites, which were beneficial for NH_3 and NH_x species formation and then followed by the well establish NH_3-SCR pathway; and the last one is the synergistic effect between Pd and Mn, which enhanced the H-spillover process and the adsorption and oxidation of nitrogen oxide, some of which adsorbed on MnO_x were easily removed by the dissociated hydrogen atom from Pd surface in the reductive atmosphere, thus leaving more active sites available on Pd.

Based upon the above discussion, the essential reaction route of the H_2-SCR of NO_x on Pd0.5Mn2 can be described as following: because reduction of these active nitrogen oxides requires the spillover of hydrogen atom (H) formed on Pd, the H_2-SCR of NO_x reaction starts with the dissociation of hydrogen over Pd surface. NO and O_2 adsorbed on MnO_x and the support are activated to form various types of nitrogen oxides species (NO_x^-), which are comparatively unstable and highly active to be reduced by hydrogen atom to produce N_2, N_2O and H_2O. Moreover, another reaction route over Pd0.5Mn2 catalyst also exists. Some of these adsorbed nitrogen oxides species (NO_x^-) react with dissociated hydrogen atom to produce gas phase NH_3 and NH_x ($x = 0–2$) species adsorbed on Lewis acid sites. And then NH_3 and NH_x species participate in the well-known reaction of NH_3-SCR. All of these contribute to the high activity and significantly high N_2 selectivity.

4. Conclusions

Mn modified Pd0.5 catalyst exhibited high activity and considerably high N_2 selectivity compared with Pd0.5 alone for the H_2-SCR of NO_x. The optimal Mn loading was 2 wt%. Even in the presence of H_2O, PdMn catalyst still showed higher catalytic performance. XPS results showed that PdO was the predominant active site for the reduction of NO_x. The co-presence of Mn and Pd induced a synergetic effect for H_2-SCR: new active nitrogen oxides adsorbed on MnO_x appeared and the removal of active nitrogen oxide adsorbed on Pd0.5Mn2 catalyst was promoted. In situ DRIFTS results revealed that more unstable nitrogen oxide species were adsorbed and activated on the catalyst due to the addition of Mn. In addition, Lewis acid sites dominantly existed on Pd0.5Mn2 catalyst at high temperature, leading to the presence of adsorbed NH_3 and NH_x species, which reduced nitrate/nitrite species at high temperatures following the well-established NH_3-SCR route. All of these contribute to the high NO_x conversion and N_2 selectivity of PdMn catalyst.

Acknowledgments

This research was financially supported by the National Natural Science Foundation of China (21377010), the Fundamental Research Funds for the Central Universities (YS1401), State Environmental Protection Key Laboratory of Sources and Control of Air Pollution Complex (SCAPC201402), and the Program for New

Century Excellent Talents of the Chinese Ministry of Education (NCET-13-0650).

Appendix A. Supplementary data

Supplementary data associated with this article can be found, in the online version, at http://dx.doi.org/10.1016/j.apcatb.2015.04.048.

References

[1] R. Burch, J.P. Breen, F.C. Meunier, Appl. Catal. B 39 (2002) 283–303.
[2] P.M. More, D.L. Nguyen, P. Granger, C. Dujardin, M.K. Dongare, S.B. Umbarkar, Appl. Catal. B 174–175 (2015) 145–156.
[3] Z. Liu, S.I. Woo, Catal. Rev. Sci. Eng. 48 (2006) 43–89.
[4] L. Zhang, L. Li, Y. Cao, X. Yao, C. Ge, F. Gao, Y. Deng, C. Tang, L. Dong, Appl. Catal. B 165 (2015) 589–598.
[5] Z. Liu, J. Li, S.I. Woo, Energy Environ. Sci. 5 (2012) 8799–8814.
[6] S. Bensaid, E.M.N. Borla, D. Russo Fino, V. Specchia, Ind. Eng. Chem. Res. 49 (2010) 10323–10333.
[7] R.C. Hahn, M. Endisch, F.J.P. Schott, S. Kureti, Appl. Catal. B 168–169 (2015) 429–440.
[8] M. Leicht, F.J.P. Schott, M. Bruns, S. Kureti, Appl. Catal. B 117–118 (2012) 275–282.
[9] C.N. Costa, A.M. Efstathiou, J. Phys. Chem. C 111 (2007) 3010–3020.
[10] G.C. Mondragón Rodríguez, B. Saruhan, Appl. Catal. B 93 (2010) 304–313.
[11] P.G. Savva, C.N. Costa, Catal. Rev. 53 (2011) 91–151.
[12] S. Yang, X. Wang, W. Chu, Z. Song, S. Zhao, Appl. Catal. B 107 (2011) 380–385.
[13] B. Wen, Fuel 81 (2002) 1841–1846.
[14] L. Li, F. Zhang, N. Guan, E. Schreier, M. Richter, Catal. Commun. 9 (2008) 1827–1832.
[15] M. Leicht, F.J.P. Schott, M. Bruns, S. Kureti, Appl. Catal. B 117–118 (2012) 275–282.
[16] G. Qi, R.T. Yang, F.C. Rinaldi, J. Catal. 237 (2006) 381–392.
[17] M. Fernández-García, A. Martínez-Arias, A. Iglesias-Juez, A.B. Hungría, J.A. Anderson, J.C. Conesa, J. Soria, J. Catal. 214 (2003) 220–233.
[18] B. Greenhalgh, J.P. Charland, M. Stanciulescu, R. Burich, J. Kelly, Catal. Today 151 (2010) 285–290.
[19] S.M. Park, M.Y. Kim, E.S. Kim, H.S. Han, G. Seo, Appl. Catal. A 1395 (2011) 120–128.
[20] C.N. Costa, V.N. Stathopoulos, V.C. Belessi, A.M. Efstathiou, J. Catal. 197 (2001) 350–364.
[21] A.J. Jaworowski, R. Ásmundsson, P. Uvdal, S.M. Gray, A. Sandell, Surf. Sci. 501 (2002) 83–92.
[22] Z. Liu, J. Li, J. Hao, Chem. Eng. J. 165 (2010) 420–425.
[23] C.N. Costa, A.M. Efstathiou, Appl. Catal. B 72 (2007) 240–252.
[24] G.G. Olympiou, A.M. Efstathiou, Chem. Eng. J. 170 (2011) 424–432.
[25] F.J.P. Schott, P. Balle, J. Adler, S. Kureti, Appl. Catal. B 87 (2009) 18–29.
[26] A. Ueda, T. Nakao, M. Azuma, T. Kobayashi, Catal. Today 45 (1998) 135–138.
[27] C.N. Costa, P.G. Savva, J.L.G. Fierro, A.M. Efstathiou, Appl. Catal. B 75 (2007) 147–156.
[28] W. Huang, Z. Zuo, P. Han, Z. Li, T. Zhao, Electron. Spectrosc. Relat. Phenom. 173 (2009) 88–95.
[29] G. Beketov, B. Heinrichs, J.P. Pirard, S. Chenakin, N. Kruse, Appl. Surf. Sci. 287 (2013) 293–298.
[30] N. Macleod, R. Cropley, J.M. Keel, R.M. Lambert, J. Catal. 221 (2004) 20–31.
[31] E. Beyreuther, S. Grafström, L.M. Eng, Phys. Rev. B 73 (2006) 155425–155434.
[32] Z. Wu, R. Jin, Y. Liu, H. Wang, Catal. Commun. 13 (2008) 2217–2220.
[33] P.R. Ettireddy, N. Ettireddy, S. Mamedov, P. Boolchand, P.G. Smirniotis, Appl. Catal. B 76 (2007) 123–134.
[34] J.M.G. Amores, V.S. Escribano, G. Ramis, G. Busca, Appl. Catal. B 13 (1997) 45–58.
[35] M. Mihaylov, K. Chakarova, K. Hadjiivanov, J. Catal. 228 (2004) 273–281.
[36] Q. Yu, M. Richter, L. Li, F. Kong, G. Wu, N. Guan, Catal. Commun. 11 (2010) 955–959.
[37] C.N. Costa, A.M. Efstathiou, J. Phys. Chem. B 108 (2004) 2620–2630.
[38] L. Chen, J. Li, M. Ge, Environ. Sci. Technol. 44 (2010) 9590–9596.
[39] L. Li, F. Zhang, N. Guan, E. Scherier, M. Richter, Catal. Commun. 9 (2008) 1827–1832.
[40] A. Satsuma, M. Hashimoto, J. Shibata, H. Yoshida, T. Hattori, Chem. Commun. (2003) 1698–1699.
[41] T. Nanba, C. Kohno, S. Masukawa, J. Uchisawa, N. Nakayama, A. Obuchi, Appl. Catal. B 46 (2003) 353–364.
[42] J. Yang, O. Fu, D. Wu, S. Wang, Appl. Catal. B 49 (2004) 61–65.
[43] J. Shibata, M. Hashimoto, K. Shimizu, J. Phys. Chem. B 108 (2004) 18327–18335.
[44] Y. Yazawa, H. Yoshida, T. Hatorri, Appl. Catal. A 237 (2002) 139–148.
[45] Y. Yazawa, H. Yoshida, N. Kataji, S. Komia, A. Satsuma, T. Hattori, J. Catal. 187 (1999) 15–23.